Late to the Table: Diversification of tetrapod mandibular biomechanics lagged behind the evolution of terrestriality

Philip S. L. Anderson[1], Matt Friedman[2], Marcello Ruta[3]

[1]Department of Biology, University of Massachusetts, Amherst, MA, USA
[2]Department of Earth Sciences, University of Oxford, Oxford OX1 3AN, UK
[3]School of Life Science, University of Lincoln, Lincoln LN6 7TS, UK

Supplementary Information

TABLE OF CONTENTS

1. Functional characters

Ten continuous biomechanical jaw traits were measured from photographs or illustrations of the lateral view of the lower jaws using the software package ImageJ (Rasband 1997-2009). We elected to use mandibular traits because we are primarily interested in the evolution and radiation of the feeding structures during this transition. While upper jaws are part of this innovation as well, examining lower jaws alone permitted a larger sample of genera.

Character descriptions.
Some of these characters are based on similar jaw metrics used in a previous studies on early gnathostomes (Anderson 2009a; Anderson et al. 2011). Schematic drawings of selected characters are given in Figure S1-S7.

C1, Anterior mechanical advantage: The vertebrate lower jaw can be modeled as a third-order lever (Barel 1983; Westneat 1994). A third-order lever is constructed such that the fulcrum (point of rotation) is at the proximal end, while the input force is applied to the middle of the lever in order to lift some load at the distal end. In a mandible, the fulcrum is the articular joint, while the input is provided by adductor mandibulae muscles and the force is transferred to the dentition to produce a bite force. The mechanical advantage (ratio of moment arms) represents the proportion of input muscle force that is applied at the dentition. This measure correlates with diet in modern fishes (Westneat 1994; Wainwright and Richard 1995). The input moment arm is measured from the joint of articulation to the center of the region of adductor insertion, identified by a distinct fossa. The output moment arm is measured from the joint to the anterior most dental tip (Figure S1). This measure represents the lowest potential mechanical advantage along the dentition.

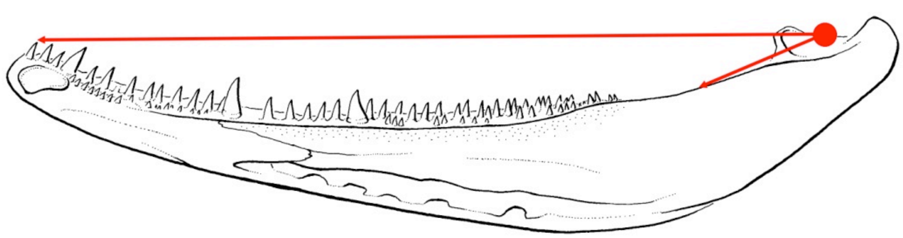

Figure S1. Measurements required for the calculation of functional character C1, anterior mechanical advantage. Mandible of *Ventastega* adapted from Ahlberg et al. (2008).

C2, Posterior mechanical advantage: The same as above, except the output moment arm is measured to the posterior-most dental surface. This measure represents the highest potential mechanical advantage along the dentition (Figure S2).

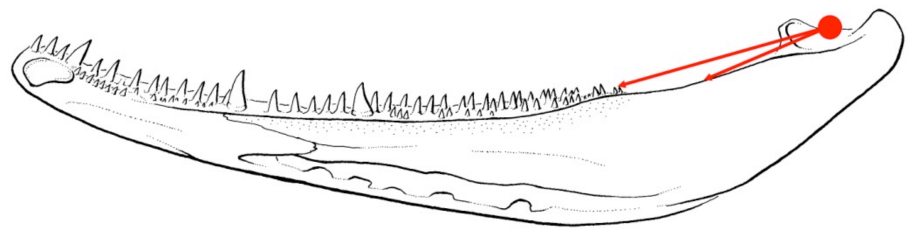

Figure S2. Measurements required for the calculation of functional character C2, posterior mechanical advantage. Mandible of *Ventastega* adapted from Ahlberg et al. (2008).

C3, Maximum jaw depth/length: The second moment of area describes how material is distributed around the centroid of a beam's cross section. It is directly proportional to the flexural stiffness of the beam (Vogel 2003). Second moment of area has been used as a metric for stiffness in chondrichthyan mandibles (Summers et al. 2004), crocodile skulls (Metzger et al. 2005) and mammalian jaws (Daegling 2001. For many of the mandibles used in this study, only lateral views are known, so precise estimates of cross-sectional profiles are not possible.

Calculating functionally relevant second moment of area requires knowledge of load orientation relative to the cross section (Vogel 2003). In general, the dimension of the cross section oriented along the axis of the load is most important and has the strongest influence on the calculated value (Vogel 2003; see the equations on page 368). For the majority of sampled mandibles, the main loads experienced will primarily be in the dorsal/ventral direction. Therefore, the depth of the jaw is a potential proxy for the flexural stiffness under dorso-ventral loads. This assumes a consistent uniform material across all jaws and a consistent width. Neither assumption is true, but most specimens do not deviate greatly from these conditions, hence these assumptions are reasonable for a comparative analysis. To determine the maximum potential stiffness, the greatest depth measurement is taken along the jaw and divided by the overall jaw length (Figure S3).

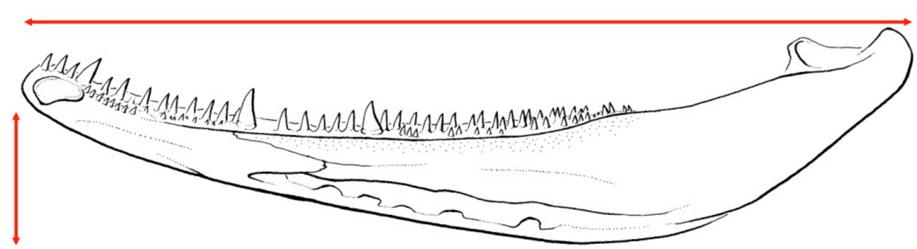

Figure S3. Measurements required for the calculation of functional character C3, ratio of jaw depth to jaw length. Mandible of *Ventastega* adapted from Ahlberg et al. (2008).

C4, Average jaw depth/length: For the average measure, the lateral area of the jaw is measured (without teeth included) and then divided by the jaw length once to discern to average jaw depth. This measure is divided by jaw length again in order to determine the average depth/length ratio.

C5, Articular offset: It has been observed in many mammalian taxa that the placement of the jaw joint relative to the tooth row has a profound effect on the occlusal pattern (Turnbull 1970; Greaves 1974; Herring 1993). If the joint lies directly in line with the dental row, the teeth will occlude like a pair of scissors, gradually coming into contact from posterior to anterior end. If, however, the joint lies off the line tangent to the tooth row, the teeth will occlude all at once, more like a wrench. Differences in occlusal pattern often relate to dietary differences in mammals and may have an effect on force vectors during biting (Ramsay and Wilga 2007). Similar variation has been identified in sharks (Ramsay and Wilga 2007) and 'placoderms' (Anderson 2008, 2009a).

Articular offset is determined by first drawing a line tangent to the dorsal surface of the jaw along the tooth or dental row. Then, a line is drawn perpendicular from the tangent which intersects the articular joint. The length of this line is divided by jaw length to estimate deviation from a pure scissor-like occlusion (Figure S4).

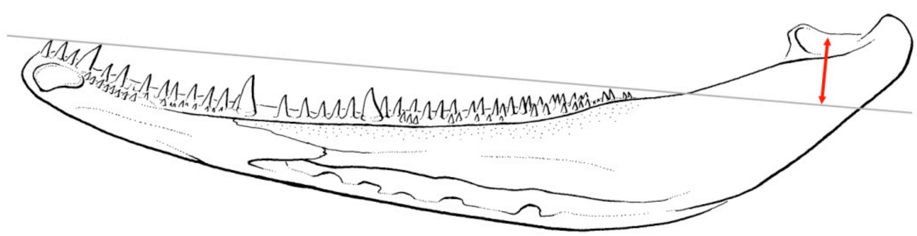

Figure S4. Measurements required for the calculation of functional character C5, articular offset. Mandible of *Ventastega* adapted from Ahlberg et al. (2008).

C6, Relative dental row length: The more of the jaw that bears dental tools, the larger the variation in potential bite force and speed. A larger dental row also allows for a greater variation in dental tools and potentially allows for greater variability of function. This measure is taken as the ratio of the length of the dental row to the overall jaw length (Figure S5).

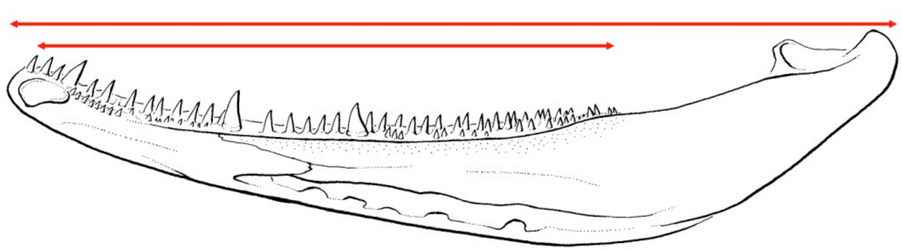

Figure S5. Measurements required for the calculation of functional character C6, relative dental row length. Mandible of *Ventastega* adapted from Ahlberg et al. (2008).

C7, Relative adductor fossa length: The force output of a muscle is directly proportional to the cross sectional area of the muscle. The length of the adductor muscle insertion area is a proxy for the cross sectional area of the muscle, and will give a sense of the variation in muscle size and strength across groups. This trait is measured as the ratio of the length of the muscle insertion area to the jaw length (Figure S6).

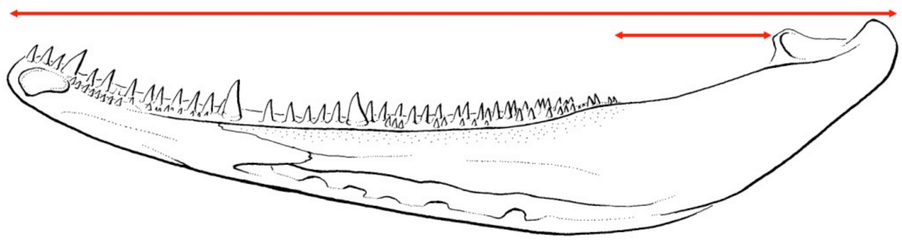

Figure S6. Measurements required for the calculation of functional character C7, relative adductor fossa length. Mandible of *Ventastega* adapted from Ahlberg et al. (2008).

C8, Tooth height/width: One of the primary roles for dentition is to create fractures in food materials. Tooth shape reflects a functional response to the toughness and material properties of food (Lucas 2004). Experimental analyses have shown that the particular shapes of dental tools can have measurable effects on the ability to cause fracture in biological materials (Evans and Sanson 1998; Anderson and LaBarbera 2008; Anderson 2009b). In particular, it has been shown that the cusp angle, taken as the volume of a cone that is forced into a material, can have a large effect on the ability to puncture flesh and/or cuticle (Evans and Sanson 1998). At the same time, a wider, more blunt tooth may be advantageous when trying to crack hard, brittle items (Lucas 2004).

The ratio of the height of a tooth to its base width acts as proxy for cusp angle. It measures how broad or narrow the tooth is, and how much dental material must be forced into a crack during puncture. The tallest tooth present is used. There is a question as to hther the difference between marginal and coronoid dentition should be taken into consideration. While these two types of dentition are important in terms of taxonomic affinity and developmental structure, mechanically speaking they perform the same task: puncturing/cutting food items. Therefore, we consider them equivalent in this study. The height of the tooth is taken from the base of the tooth up to the tip, perpendicular to the dorsal jaw surface. The base is the full width of the tooth base.

C9, Tooth height/jaw depth: The taller and larger the teeth are relative to the rest of the jaw, the more effective they are at holding or slicing prey. The ratio of the tooth height to the jaw depth calculates how tall the teeth are relative to the jaw. Tooth height is measured as for C8 and the average jaw depth is the same as measured for C4.

C10, Relative symphyseal length: The symphysis of the vertebrate jaws undergoes a unique set of forces and stresses. Previous studies have shown that both the relative size of the symphysis will affect how well it can withstand certain shear stresses and torsion (Daegling 2001; Walmsley et al. 2012). As a proxy for the mechanics of the symphysis, this character measures its relative length in comparison with the rest of the jaw. The symphyseal length is taken as the longest dimension that can be measured along the cross section of the union of the two jaw halves (symphyseal section) (Figure S7). This line shows different orientations with respect to the long axis of the jaw in different taxa. In order to obtain the functional metric, the symphseal length is dived by overall jaw length.

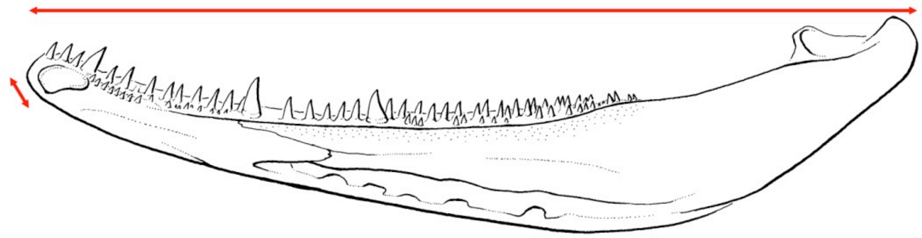

Figure S7. Measurements required for the calculation of functional character C10, relative symphyseal length. Mandible of *Ventastega* adapted from Ahlberg et al. (2008).

2. Multivariate analysis

Summary statistics for the biomechanical phylogenetic principal components analysis.

Table S1. Eigenvalues and relative variance of the phylogenetic PCA.

	Eigenvalues	%Variance
PC1	2.424358	24.2435793
PC2	1.896067	18.9606695
PC3	1.436842	14.3684196
PC4	1.288104	12.8810397
PC5	0.9594741	9.5947407
PC6	0.8059777	8.0597768
PC7	0.5544939	5.5449389
PC8	0.4363867	4.3638669
PC9	0.1058172	1.058172
PC10	0.09247967	0.9247967

Tables S2-S3. Loadings of the 10 biomechanical characters onto PCs 1-10.

	C1	C2	C3	C4	C5
PC1	0.0011	-0.1968	-0.9222	-0.9166	0.2946
PC2	-0.8939	-0.3690	0.0885	-0.1063	-0.1101
PC3	-0.3057	-0.4219	0.1604	0.0598	0.5619
PC4	0.1899	0.7689	-0.0785	-0.1503	0.1986
PC5	-0.0749	0.0221	-0.0478	-0.1455	0.1020
PC6	0.0385	0.0409	0.0412	-0.0052	0.7129
PC7	-0.0668	0.1507	0.1510	0.1163	0.0269
PC8	-0.1168	0.0400	-0.1919	-0.2048	-0.1613
PC9	0.2103	-0.1620	0.0727	-0.0805	-0.0173
PC10	0.0436	-0.0562	-0.2023	0.1979	0.0143

	C6	C7	C8	C9	C10
PC1	-0.2083	-0.4056	-0.2114	-0.0316	-0.5954
PC2	0.7569	-0.5545	-0.0372	0.0123	0.2181
PC3	-0.1010	0.3772	0.5070	0.5345	-0.3537
PC4	0.4850	-0.1889	0.3480	0.4479	0.0090
PC5	0.0437	0.3420	-0.6729	0.5049	0.3048
PC6	0.1041	0.0254	-0.0809	-0.4420	0.2819
PC7	0.2590	0.1605	-0.2842	-0.1580	-0.5401
PC8	0.1703	0.4545	0.1887	-0.1911	0.0931
PC9	0.1515	0.0052	0.0049	0.0167	-0.0023
PC10	0.0807	0.0063	-0.0062	0.0227	0.0028

3. Measurements of functional disparity

Table S4. Disparity measures for sampled taxa, divided across six time bins. Values in parentheses below disparity measures represent 95% confidence intervals obtained from taxonomic bootstrapping.

	Early-Mid Devonian	Late Devonian	Mississippian	Early Pennsylvanian	Late Pennsylvanian	early Permian
Sum of ranges	67.862 (47.49-81.89)	80.31 (69.75-89.45)	104.63 (90.306-115.364)	119.707 (104.533-130.99)	118.899 (93.379-136.196)	129.3 (109.08-143.78)
Product of ranges	5.714 (3.734-7.037)	7.179 (6.165-7.937)	9.626 (8.35-10.656)	10.984 (9.467-12.151)	10.31 (8.114-11.875)	10.879 (9.391-12.105)
Maximum distance	18.694 (15.287-19.54)	20.182 (15.95-22.139)	22.362 (19.54-23.591)	26.662 (20.833-29.439)	28.758 (21.601-29.413)	33.487 (26.785-35.814)
Area of convex hull	65.305 (0-111.657)	84.208 (39.672-110.01)	100.001 (45.733-137.21)	191.356 (120.02-255.96)	203.827 (68.143-306.38)	263.704 (123.37-369.82)
PCA volume	56.817 (37.979-80.194)	41.172 (27.44-60.597)	43.406 (30.263-61.956)	45.974 (31.799-69.153)	72.727 (43.241-115.36)	99.213 (56.179-155.13)
Sum of variances	96.338 (57.636-123.51)	81.194 (62.038-99.912)	103.239 (78.938-127.66)	110.701 (86.77-137.58)	148.847 (96.138-204.14)	192.315 (131.58-251.01)
Product of variances	5.342 (2.321-7.695)	5.262 (3.939-6.407)	7.613 (5.953-9.121)	7.728 (6.054-9.496)	8.929 (5.957-11.836)	10.204 (8.131-11.802)
Mean pairwise distance	12.561 (8.8-14.867)	11.912 (10.258-13.242)	13.538 (11.759-15.133)	14.019 (12.462-15.579)	15.875 (12.889-18.757)	18.163 (15.086-20.776)
Median pairwise distance	14.218 (10.497-16.176)	12.483 (11.082-13.954)	14.108 (11.951-15.881)	14.151 (12.54-15.645)	15.689 (12.953-19.967)	17.972 (14.693-22.068)
Mean distance to the centroid	8.783 (6.319-10.216)	8.453 (7.285-9.476)	9.554 (8.297-10.732)	9.939 (8.82-11.098)	11.149 (9.104-13.345)	12.836 (10.647-14.921)

4. Statistical tests of group separation in morphospace

Table S5. Comparison of the distributions of stratigraphically binned groups in morphospace, using an analysis of similarities (ANOSIM). Cells highlighted in pink indicate significant differences after Bonferroni correction.

ANOSIM: R = 0.09053, p = 0.0023
Post-hoc pairwise tests (p\R)

	E-M Devonian	L Devonian	Mississippian	E Pennsylvanian	L Pennsylvanian	e Permian
E-M Devonian		0.08088	0.1778	0.2539	0.08712	-0.016
L Devonian	1		0.1205	0.1469	0.1389	0.1705
Mississippian	0.9795	0.1635		-0.01873	0.008384	0.06669
E Pennsylvanian	0.315	0.2025	1		0.05494	0.1638
L Pennsylvanian	1	0.0705	1	1		-0.02526
e Permian	1	**0.021**	0.5055	0.099	1	

Table S6. Comparison of the distributions of stratigraphically binned groups in morphospace, using a non-parametric multivariate analysis of variance (NPMANOVA). Cells highlighted in pink indicate significant differences after Bonferroni correction.

NPMANOVA: F = 2.594, p = 0.0001
Post-hoc pairwise tests (p\F)

	E-M Devonian	L Devonian	Mississippian	E Pennsylvanian	L Pennsylvanian	e Permian
E-M Devonian		1.424	2.587	3.648	2.462	2.095
L Devonian	1		3.586	5.322	4.369	5.474
Mississippian	0.1335	**0.027**		0.4414	0.9444	2.22
E Pennsylvanian	**0.0495**	**0.0015**	1		1.117	3.366
L Pennsylvanian	0.309	**0.006**	1	1		0.863
e Permian	0.894	**0.0165**	0.6675	0.1245	1	

Table S7. Comparison of the distributions of taxonomic assemblages in morphospace, using an analysis of similarities (ANOSIM). Cells highlighted in pink indicate significant differences after Bonferroni correction**.**

ANOSIM: R = 0.1107, p = 0.0001

Post-hoc pairwise tests (p\R)

	Tetrapodomorph fishes	Post-'elpistostegalian' stem tetrapods	Lepospondyls	Temnospondyls	Total-group amniotes
Fishes		0.2155	0.1232	0.3445	0.06708
Stem tetrapods	**0.003**		0.2753	0.08927	0.1192
Lepospondyls	**0.041**	**0.002**		0.1499	-0.01446
Temnopondyls	**0.001**	0.535	0.066		-0.01096
Amniotes	0.64	0.16	1	1	

Table S8. Comparison of the distributions of taxonomic assemblages in morphospace, using a non-parametric multivariate analysis of variance (NPMANOVA). Cells highlighted in pink indicate significant differences after Bonferroni correction.

NPMANOVA: F = 3.63, p = 0.0001
Post-hoc pairwise tests (p\F)

	Tetrapodomorph fishes	Post-'elpistostegalian' stem tetrapods	Lepospondyls	Temnospondyls	Total-group amniotes
Fishes		6.053	2.701	5.448	2.322
Stem tetrapods	**0.001**		6.517	2.171	6.367
Lepospondyls	0.1	**0.001**		3.111	1.073
Temnopondyls	**0.001**	0.333	0.082		2.673
Amniotes	0.392	**0.002**	1	0.298	

5. Statistical tests for differences in rates of functional evolution

Table S8. Results of bootstrap tests (two-tailed) for differences in rates of functional evolution between different domains of tetrapod phylogeny.

Comparison	***p* (PC1)**	***p* (PC2)**
Crown amniotes plus diadectids versus all remaining taxa	**0.0166**	0.2228
Total-group amniotes versus all remaining taxa	0.1562	0.2602
Digited tetrapods versus ‘fishes’	0.3046	0.2228

6. First appearance data (FAD) for selected taxa

Table S9. Absolute ages (in Myr) for first appearance data (FAD) of the taxa used in this work

Taxon	FAD
Tungsenia	409.2
Kenichthys	400.45
Letognathus	352.8
Rhizodus	336.55
Gyroptychius	390.5
Gogonasus	383.9
Osteolepis	390.5
Cladarosymblema	336.55
Ectosteorhachis	298.4
Megalichthys	336.55
Medoevia	364.16
Spodichthys	383.9
Tristichopterus	387.2
Eusthenopteron	387.2
Platycephalichthys skuenicus	367.5
Platycephalichthys bischoffi	383.9
Panderichthys	387.2
Tiktaalik	383.9
Ventastega	362.4
Acanthostega	367.5
Ymeria	367.5
Metaxygnathus	367.5
Ichthyostega	367.5
Densignathus	362.4
Elginerpeton	376.9
Whatcheeria	336.55
Acherontiscus	327.1
Adelogyrinus	325.1
Adelospondylus	314.1
Greererpeton	321
Colosteus	308.6
Crassigyrinus	330.3
Doragnathus	325.1
Sigournea	336.55
Spathicephalus	325.1
Baphetes	314.1
Megalocephalus	314.1
Caerorhachis	327.1
Silvanerpeton	332.2
Eoherpeton	330.3
Proterogyrinus	325.1
Pholiderpeton attheyi	314.1
Anthracosaurus	314.1

Neopteroplax	306
Pholiderpeton scutigerum	314.1
Gephyrostegus	308.6
Utegenia	298.4
Discosauriscus	298.4
Westlothiana	332.2
Oestocephalus	314.1
Coloraderpeton	306
Sauropleura	308.6
Batrachiderpeton	314.1
Diploceraspis	298.4
Diplocaulus	306
Microbrachis	308.6
Hyloplesion	308.6
Crinodon	308.6
Asaphestera	314.1
Tuditanus	308.6
Batropetes	298.4
Brachydectes	308.6
Limnoscelis	306
Desmatodon	306
Diadectes	298.4
Archaeovenator	302.35
Aerosaurus	298.4
Ophiacodon	298.4
Ianthasaurus	306
Edaphosaurus	298.4
Haptodus	306
Sphenacodon	298.4
Brouffia	308.6
Paleothyris	308.6
Cephalerpeton	308.6
Petrolacosaurus	306
Adamanterpeton	308.6
Cochleosaurus	308.6
Eryopid	302.25
Eryops	298.4
Iberospondylus	302.25
Capetus	308.6
Sclerocephalus	298.4
Archegosaurus	295.4
Balanerpeton	332.2
Dendrerpeton	314.1
Erpetosaurus	308.6
Trimerorhachis	298.4
Limnogyrinus	308.6

7. Time-calibrated tree, readable in R

```
#NEXUS

BEGIN TAXA;
      DIMENSIONS NTAX = 89;
      TAXLABELS
            Tungsenia
            Kenichthys
            Letognathus
            Rhizodus
            Gogonasus
            Gyroptychius
            Osteolepis
            Medoevia
            Cladarosymblema
            Ectosteorhachis
            Megalichthys
            Spodichthys
            Tristichopterus
            Eusthenopteron
            Platycephalichthys_skuenicus
            Platycephalichthys_bischoffi
            Panderichthys
            Tiktaalik
            Ventastega
            Acanthostega
            Ymeria
            Metaxygnathus
            Ichthyostega
            Densignathus
            Elginerpeton
            Whatcheeria
            Greererpeton
            Colosteus
            Acherontiscus
            Adelogyrinus
            Adelospondylus
            Crassigyrinus
            Doragnathus
            Sigournea
            Spathicephalus
            Baphetes
            Megalocephalus
            Caerorhachis
            Adamanterpeton
            Cochleosaurus
            Balanerpeton
            Dendrerpeton
            Limnogyrinus
            Erpetosaurus
            Trimerorhachis
            Iberospondylus
            Eryopid
```

```
		Eryops
		Capetus
		Sclerocephalus
		Archegosaurus
		Silvanerpeton
		Eoherpeton
		Proterogyrinus
		Pholiderpeton_scutigerum
		Pholiderpeton_attheyi
		Anthracosaurus
		Neopteroplax
		Gephyrostegus
		Utegenia
		Discosauriscus
		Westlothiana
		Oestocephalus
		Coloraderpeton
		Sauropleura
		Batrachiderpeton
		Diploceraspis
		Diplocaulus
		Microbrachis
		Hyloplesion
		Batropetes
		Brachydectes
		Crinodon
		Asaphestera
		Tuditanus
		Limnoscelis
		Desmatodon
		Diadectes
		Brouffia
		Paleothyris
		Cephalerpeton
		Petrolacosaurus
		Ophiacodon
		Archaeovenator
		Aerosaurus
		Ianthasaurus
		Edaphosaurus
		Haptodus
		Sphenacodon
	;
END;

BEGIN TREES;
	TRANSLATE
		1	Tungsenia,
		2	Kenichthys,
		3	Letognathus,
		4	Rhizodus,
		5	Gogonasus,
		6	Gyroptychius,
		7	Osteolepis,
		8	Medoevia,
```

```
Cladarosymblema,
Ectosteorhachis,
Megalichthys,
Spodichthys,
Tristichopterus,
Eusthenopteron,
Platycephalichthys_skuenicus,
Platycephalichthys_bischoffi,
Panderichthys,
Tiktaalik,
Ventastega,
Acanthostega,
Ymeria,
Metaxygnathus,
Ichthyostega,
Densignathus,
Elginerpeton,
Whatcheeria,
Greererpeton,
Colosteus,
Acherontiscus,
Adelogyrinus,
Adelospondylus,
Crassigyrinus,
Doragnathus,
Sigournea,
Spathicephalus,
Baphetes,
Megalocephalus,
Caerorhachis,
Adamanterpeton,
Cochleosaurus,
Balanerpeton,
Dendrerpeton,
Limnogyrinus,
Erpetosaurus,
Trimerorhachis,
Iberospondylus,
Eryopid,
Eryops,
Capetus,
Sclerocephalus,
Archegosaurus,
Silvanerpeton,
Eoherpeton,
Proterogyrinus,
Pholiderpeton_scutigerum,
Pholiderpeton_attheyi,
Anthracosaurus,
Neopteroplax,
Gephyrostegus,
Utegenia,
Discosauriscus,
Westlothiana,
Oestocephalus,
```

```
        64    Coloraderpeton,
        65    Sauropleura,
        66    Batrachiderpeton,
        67    Diploceraspis,
        68    Diplocaulus,
        69    Microbrachis,
        70    Hyloplesion,
        71    Batropetes,
        72    Brachydectes,
        73    Crinodon,
        74    Asaphestera,
        75    Tuditanus,
        76    Limnoscelis,
        77    Desmatodon,
        78    Diadectes,
        79    Brouffia,
        80    Paleothyris,
        81    Cephalerpeton,
        82    Petrolacosaurus,
        83    Ophiacodon,
        84    Archaeovenator,
        85    Aerosaurus,
        86    Ianthasaurus,
        87    Edaphosaurus,
        88    Haptodus,
        89    Sphenacodon
    ;
    TREE * UNTITLED = [&R]
(1:13.8,(2:11.275,((3:18.85,4:35.1):35.83,((5:15.09,(6:4.245,(7:2.1225,(8:
14.23125,((10:52.09708333,11:13.94708333):13.94708333,9:27.89416667):13.94
708333):14.23125):2.1225):4.245):4.245,((12:11.3175,(13:4.00875,(14:2.0043
75,15:21.704375):2.004375):4.00875):4.00875,(16:11.3175,(17:4.00875,(18:3.
654375,(19:23.63232143,(20:17.01026786,((21:4.7,22:4.7):10.78821429,((23:1
2.44410714,(24:16.02205357,25:1.522053571):1.522053571):1.522053571,(26:22
.45808036,(((27:3.05,28:15.45):9.35,(29:3.15,(30:2.575,31:13.575):2.575):3
.15):21.86506696,(32:21.22205357,(((33:15.19301339,34:3.743013393):3.74301
3393,(35:9.468013393,(36:10.2340067,37:10.2340067):10.2340067):9.468013393
):3.743013393,(38:18.45346301,(((39:11.8,40:11.8):20.70230867,(((41:2.2255
77168,42:20.32557717):2.225577168,(43:14.02557717,(44:7.012788584,45:17.21
278858):7.012788584):14.02557717):2.225577168,((46:3.175,(47:1.5875,48:5.4
375):1.5875):23.35948767,(49:10.09224384,(50:10.14612192,51:13.14612192):1
0.14612192):10.09224384):10.09224384):2.225577168):2.225577168,((52:3.7092
95281,(53:2.80464764,(54:4.00232382,(55:7.50116191,(56:3.750580955,(57:1.8
75290478,58:9.975290478):1.875290478):3.750580955):7.50116191):4.00232382)
:2.80464764):3.709295281,(59:29.53487245,((60:16.9,61:16.9):21.35115434,((
62:1.483718112,(((63:4.895929528,64:12.99592953):4.895929528,(65:12.027906
04,(66:3.263953019,(67:13.28197651,68:5.681976509):5.681976509):3.26395301
9):3.263953019):4.895929528,((69:2.75,70:2.75):14.50023087,((71:12.95,72:2
.75):11.56267315,(73:11.37511543,(74:2.937557717,75:8.437557717):2.9375577
17):2.937557717):2.937557717):2.937557717):4.895929528):1.483718112,((76:1
.3,(77:0.65,78:8.25):0.65):21.22557717,((79:6.641859056,(80:3.320929528,(8
1:1.660464764,82:4.260464764):1.660464764):3.320929528):6.641859056,((83:6
.383333333,(84:1.216666667,85:5.166666667):1.216666667):13.12945525,((86:3
.970929528,87:11.57092953):3.970929528,(88:3.970929528,89:11.57092953):3.9
70929528):3.970929528):3.970929528):6.641859056):6.641859056):1.483718112)
```

```
:1.483718112):1.483718112):3.709295281):2.225577168):2.225577168):3.743013
393):3.743013393):3.743013393):22.45808036):1.522053571):1.522053571):1.52
2053571):1.522053571):3.654375):4.00875):4.00875):4.00875):4.245):4.245):1
1.275);
END;
```

8. Supplementary references

Ahlberg PE, Clack JA, Lukševičs E, Blom H, Zupinš I. *Ventastega curonica* and the origin of tetrapod morphology. Nature 2008;453:1199-1204.

Anderson PSL. Shape variation between arthrodire morphotypes indicates possible feeding niches. J Vert Paleont 2008;28:961-969.

Anderson PSL. Biomechanics, functional patterns, and disparity in Late Devonian arthrodires. Paleobiology 2009a;35:321-342.

Anderson PSL. The effects of trapping and blade angle of notched dentitions on fracture of biological tissues. J. Exp. Biol. 2009b;212:3627-3632.

Anderson PSL, LaBarbera M. Functional consequences of tooth design: effects of blade shape on energetics of cutting. J Exp Biol 2008;211:3619-3626.

Anderson PSL, Friedman M, Brazeau MD, Rayfield EJ. Initial radiation of jaws demonstrated stability despite faunal and environmental change. Nature 2011;476:206-209.

Barel CDN. Toward a constructional morphology of cichlid fishes (Teleostei, Perciformes). Nether J Zool 1983;33:357-424.

Daegling DJ. Biomechanical scaling of the hominid mandibular symphysis. J Morph 2001;250:12-23.

Evans AR, Sanson GD. The effect of tooth shape on the breakdown of insects. J Zool Soc Lond 1998;246:391-400.

Greaves WS. Functional implications of mammalian jaw joint position. Form Funct 1974;7:363-376.

Herring SW. Functional morphology of mammalian mastication. Amer Zool 1993;33:289-299.

Lucas PW. *Dental Functional Morphology* Cambridge University Press, Cambridge, UK, 2004.

Metzger KA, Daniel W, Ross CF. Comparison of beam theory and finite-element analysis to *in vivo* bone strain in the alligator cranium. Anat Rec 2005;283A:331-348.

Ramsay JB, Wilga CD. Morphology and mechanics of the teeth and jaws of White-Spotted Bamboo Sharks (*Chiloscyllium plagiosum*). J Morph 2007;268:664-682.

Rasband WS. ImageJ, U. S. National Institutes of Health, Bethesda, Maryland, USA, http://rsb.info.nih.gov/ij/, 1997-2009.

Summers AP, Ketcham RA, Rowe T. Structure and function of the Horn Shark (*Heterodontus francisci*) Cranium through ontogeny: development of a hard prey specialist. J Morph 2004;260:1-12.

Turnbull WD. Mammalian masticatory apparatus. Fieldiana (Geol) 1970;18:147-356.

Vogel S. *Comparative Biomechanics: Life's Physical World* Princeton University Press, Princeton, NJ, 2003.

Wainwright PC, Richard BA. Predicting patterns of prey use from morphology with fishes. Environ Biol Fish 1995;44:97-113.

Walmsley CW, Smits PD, Quayle MR, McCurry MR, Richards HS, Oldfield CC, Wroe S, Clausen PD, McHenry CR. Why the long face? The mechanics of mandibular symphysis proportion in crocodiles. PLoS ONE 2013;8:e53873

Westneat MW. Transmission of force and velocity in the feeding mechanisms of labrid fishes (Teleostei, Perciformes). Zoomorphology 1994;114:103-118.

9. Specimen references

Ahlberg PE, Clack JA. Lower jaws, lower tetrapods – a review based on the Devonian genus *Acanthostega*. T Roy Soc Edin Earth Sci 1998;89:11-46.

Ahlberg PE, Clack JA, Lukševičs E, Blom H, Zupinš I. *Ventastega curonica* and the origin of tetrapod morphology. Nature 2008;453:1199-1204.

Ahlberg PE, Friedman M, Blom H. New light on the earliest known tetrapod jaw. J Vert Paleont 2005;25:720-724.

Anderson JS. Cranial anatomy of *Coloraderpeton brilli*, postcranial anatomy of *Oestocephalus amphiuminus*, and reconsideration of Ophiderpetontidae (Tetrapoda: Lepospondyli: Aistopoda). J Vert Paleont 2003;23:532-543.

Andrews SM, Carroll RL. The Order Adelospondyli: Carboniferous lepospondyl amphibians. Trans Roy Soc Edin 1991;82:239-275.

Beaumont EH. Cranial Morphology of the Loxommatidae (Amphibia: Labyrinthodontia). Phil Trans Roy Soc Lond B 1977;280:29-101.

Beaumont EH, Smithson TR. The cranial morphology and relationships of the aberrant Carboniferous amphibian *Spathicephalus mirus* Watson. Zool J Linn Soc 1998;122:187-209.

Beerbower JR. Morphology, paleoecology, and phylogeny of the Permo-Pennsylvanian amphibian *Diploceraspis*. Bull Mus Comp Zool 1963;130:31-108.

Berman DS, Reisz RR, Scott D. Redescription of the skull of *Limmoscelis paludi*s Williston (Diadectomorpha: Limnoscelidae) from the Pennsylvanian of Canon del Cobre, northern New Mexico. In: Lucas SG, Schneider JW, Spielmann JA, editors. *Carboniferous-Permian Transition in Canon del Cobre, Northern New Mexico*. New Mexico Mus Nat His Sci Bull 2010;49:185-210.

Berman DS, Sumida SS. New cranial material of the rare diadectid *Desmatodon herperis* (Diadectomorpha) from the Late Pennsylvanian of Central Colorado. Ann Carn Mus 1995;64:315-336.

Bolt JR, Lombard RE. The mandible of the primitive tetrapod *Greererpeton*, and the early evolution of the tetrapod lower jaw. J Paleont 2001;75:1016-1042.

Bolt JR, Lombard RE. *Sigournea multidentata*, a new stem tetrapod from the Upper Mississippian of Iowa, USA. J Paleont 2006;80:717-725.

Bolt JR, Rieppel O. The holotype skull of *Llistrofus pricei* (Microsauria: Hapsidopareiontidae). J Paleont 2009;83:471-483.

Brazeau M. A new genus of rhizodontid (Sarcopterygii, Tetrapodomorpha) from the Lower Carboniferous Horton Bluff Formation of Nova Scotia, and the evolution of the lower jaws in this group. Can J Earth Sci 2005;42:1481-1499.

Carroll RL. A Middle Pennsylvanian captorhinomorph, and the interrelationships of primitive reptiles. J Paleont 1969a;43:151-170.

Carroll RL. A new family of Carboniferous amphibians. Palaeontology 1969b;12:537-548.

Carroll RL. *Batropetes* from the Lower Permian of Europe – a microsaur, not a reptile. J Vert Paleont 1991;11:229-242.

Carroll RL. Cranial anatomy of ophiderpetontid aistopods: Palaeozoic limbless amphibians. Zool J Linn Soc 1998;122:143-166.

Carroll RL, Baird D. The Carboniferous amphibian *Tuditanus* [*Eosaurus*] and the distinction between microsaurs and reptiles. Amer Mus Nov 1968;2337:1-50.

Carroll RL, Baird D. Carboniferous stem-reptiles of the family Romeriidae. Bull Mus Comp Zool 1972;143:321-364.

Carroll RL, Gaskill P. The Order Microsauria. Mem Am Phil Soc 1978;126:1-211.

Chang MM, Zhu M. A new Middle Devonian osteolepid from Qujing, Yunnan. Mem. Assoc. Australas. Palaeontolog. 1993;15:183-198.

Clack JA. *Pholiderpeton scutigerum* Huxley, an amphibian from the Yorkshire Coal Measures. Phil Trans Roy Soc Lond B 1987a;318:1-107.

Clack JA. Two new specimens of *Anthracosaurus* (Amphibia: Anthracosauria) from the Northumberland Coal Measures. Palaeontology 1987b;30:15-26.

Clack JA, Ahlberg PE, Blom H, Finney SM. A new genus of Devonian tetrapod from north-east Greenland, with new information on the lower jaw of *Ichthyostega*. Palaeontology 2012;55:73-86

Daeschler EB. Early tetrapod jaws from the Late Devonian of Pennsylvania, USA. J. Paleont. 2000;74:301-308.

Daeschler EB, Shubin NH, Jenkins FA. A Devonian tetrapod-like fish and the evolution of the tetrapod body plan. Nature 2006;440:757-763.

Douthitt H. The structure and relationships of *Diplocaulus*. Contr Walker Mus 1917;2:1-47.

Fox RC, Campbell KSW, Barwick RE, Long JA. A new osteolepiform fish from the lower Carboniferous Raymond Formation, Drummond Basin, Queensland. Mem Queensl Mus 1995;38:97-221.

Holmes RB. The Carboniferous amphibian *Proterogyrinus scheelei* Romer, and the early evolution of tetrapods. Phil Trans Roy Soc Lond B 1984;306:431-524.

Holmes RB, Carroll RL, Reisz RR. The first articulated skeleton of *Dendrerpeton acadianum* (Temnospondyli, Dendrerpetontidae) from the Lower Pennsylvanian locality of Joggins, Nova Scotia, and a review of its relationships. J Vert Paleont 1998;18:64-79.

Hook RW. *Colosteus scutellatus* (Newberry), a primitive temnospondyl amphibian from the Middle Pennsylvanian of Lincoln, Ohio. Amer Mus Nov 1983;2770:1-41.

Jeffery JE. Mandibles of rhizodontids: anatomy, function and evolution within the tetrapod stem-group. Trans Roy Soc Edin Earth Sci 2002;93:255-276.

Klembara J. The cranial anatomy of *Discosauriscus* Kuhn, a seymouriamorph tetrapod from the Lower Permian of the Boskovice Furrow (Czech Republic). Phil Trans Roy Soc Lond B 1997;352:257-302.

Klembara J , Ruta M. The seymouriamorph tetrapod *Utegenia shpinari* from the ?Upper Carboniferous-Lower Permian of Kazakhstan. Part I: Cranial anatomy and ontogeny. Trans Roy Soc Edin Earth Sci 2004;94:45-74.

Laurin M. Anatomy and relationships of *Haptodus garnettensis*, a Pennsylvanian synapsid from Kansas. J Vert Paleont 1993;13:200-229.

Laurin M, Soler-Gijón R. The oldest known stegocephalian (Sarcopterygii: Temnospondyli) from the Spain. J Vet Paleont 2006;26:284-299.

Lebedev OA. Morphology of a new osteolepidid fish from Russia. Bull Mus nat Hist natur Paris C (4) 1995;17:287-341.

Lombard RE, Bolt JR. The mandible of *Whatcheeria deltae*, an early tetrapod from the Late Mississippian of Iowa. In: Carrano MT, Gaudin TJ, Blob RW, Wible JR, editors. *Amniote Paleobiology. Perspectives on the Evolution of Mammals, Birds and Reptiles.* Chicago: Chicago University Press; 2006. p. 21-52.

Long JA, Barwick RE, Campbell KSW. Osteology and functional morphology of the osteolepiform fish *Gogonasus andrewsae* Long, 1985, from the Upper Devonian Gogo Formation, Western Australia. Rec. West. Aust. Mus. Suppl. 1997;53:1-89.

Lu J, Zhu M, Long JA, Zhao W, Senden TJ, Jia L, Qiao T. The earliest known stem-tetrapod from the Lower Devonian of China. Nature Comm 2012;3:1160.

Milner AC. A review of the Nectridea (Amphibia). In: Panchen AL, editor. *The Terrestrial Environment and the Origin of Land Vertebrates*. London: Academic Press; 1980. p. 377-405.

Milner AR, Schoch RR. *Trimerorhachis* from the Lower Permian of Texas and New Mexico: Cranial osteology, taxonomy and biostratigraphy. Fossil Rec in press.

Milner AR, Sequeira SEK. The temnospondyl amphibians from the Viséan of East Kirkton, West Lothian, Scotland. Trans Roy Soc Edin Earth Sci 1994;84:331-361.

Milner AR, Sequeira SEK. A cochleosaurid temnospondyl amphibian from the Middle Pennsylvanian of Linton, Ohio, U.S.A. Zool J Linn Soc 1998;122:261-290.

Milner AR, Sequeira SEK. Revision of the amphibian genus *Limnerpeton* (Temnospondyli) from the Upper Carboniferous of the Czech Republic. Acta Palaeont Polon 2003;48:123-141.

Milner AR, Sequeira SEK. The amphibian *Erpetosaurus radiatus* (Temnospondyli, Dvinosauria) from the Middle Pennsylvanian of Linton, Ohio: morphology and systematic position. In: Barrett PM, Milner AR, editors. *Studies on Fossil Tetrapods.* Spec Pap Palaeont 86. London: The Palaeontological Association; 2011. p. 57-73.

Panchen AL. The skull and skeleton of *Eogyrinus attheyi* Watson (Amphibia: Labyrinthodontia). Phil Trans Roy Soc Lond B 1972;263:279-326.

Panchen AL. A new genus and species of anthracosaur amphibian from the Lower Carboniferous of Scotland and the status of *Pholidogaster pisciformis* Huxley. Phil Trans Roy Soc Lond B 1975;269:581-637.

Reisz RR. *Petrolacosaurus*, the oldest known diapsid reptile. Science 1977;196:1091-1093.

Reisz RR, Berman DS. *Ianthasaurus hardestii* n. sp., a primitive edaphosaur (Reptilia, Pelycosauria) from the Upper Pennsylvanian Rock Lake Shale near Garnett, Kansas. Can J Earth Sci 1986;23:77-91.

Reisz RR, Dilkes DW. *Archaeovenator hamiltonensis*, a new varanopid (Synapsida: Eupelycosauria) from the Upper Carboniferous of Kansas. Can J Earth Sci 2003;40:667-678.

Romer AS. The larger embolomerous amphibians of the American Carboniferous. Bull Mus Comp Zool 1963;128:415-454.

Romer AS, Price LW. Review of the Pelycosauria. Geol Soc Am Spec Pap 1940;28:1-538.

Ruta M, Clack JA. A review of *Silvanerpeton miripedes*, a stem amniote from the Lower Carboniferous of East Kirkton, West Lothian, Scotland. Trans Roy Soc Edin Earth Sci 2006;97:31-63.

Ruta M, Milner AR, Coates MI. The tetrapod *Caerorhachis bairdi* Holmes and Carroll from the Lower Carboniferous of Scotland. Trans Roy Soc Edin Earth Sci 2001;92:229-261.

Sawin HJ. The cranial anatomy of *Eryops megacephalus*. Bull Mus Comp Zool 1941;88:407-463.

Schoch RR, Witzmann F. Osteology and relationships of the temnospondyl *Sclerocephalus*. Zool J Linn Soc 2009;157:135-168.

Sequeira SEK. The skull of *Cochleosaurus bohemicus* Fric, a temnospondyl from the Czech Republic (Upper Carboniferous) and cochleosaurid interrelationships. Trans Roy Soc Edin Earth Sci 2004;94:21-43.

Sequeira SEK, Milner AR. The temnospondyl amphibian *Capetus* from the Upper Carboniferous of the Czech Republic. Palaeontology 1993;36:657-680.

Smithson TR. A new labyrinthodont amphibian from the Carboniferous of Scotland. Palaeontology 1980;23:915-923.

Smithson TR, Carroll RL, Panchen AL, Andrews SM. *Westlothiana lizziae* from the Visean of East Kirkton, West Lothian, Scotland, and the amniote stem. Trans Roy Soc Edin Earth Sci 1993;84:383-412.

Snitting D. A redescription of the anatomy of the Late Devonian *Spodichthys buetleri* Jarvik, 1985 (Sarcopterygii, Tetrapodomorpha) from East Greenland. J Vert Paleont 2008;28:637-655.

Thomson KS. Revised generic diagnoses of the fossil fishes *Megalichthys* and *Ectosteorhachis* (family Osteolepidae). Bull Mus Comp Zool 1964;131:285-311.

Vallin G, Laurin M. Cranial morphology and affinities of *Microbrachis*, and a reappraisal of the phylogeny and lifestyle of the first amphibians. J Vert Paleont 2004;24:56-72.

Vorobyeva EI. Rhizodont fishes from the Main Devonian Field of the USSR. Trudy Paleontol Inst Akad Nauk SSR 1962;94:1-139. [in Russian]

Watson DMS. Croonian Lecture: the evolution and origin of the Amphibia. Phil Trans Roy Soc Lond B 1926;214:189-257.

Welles SP. The mandible of a diadectid cotylosaur. Univ Cal Publ Bull Dept Geol Sci 1941;25:423-432.

Wellstead CF. Taxonomic revision of the Lysorophia, Permo-Carboniferous lepospondyl amphibians. Bull Am Mus Nat His 1991;209:1-90

Witzmann F. Cranial morphology and ontogeny of the Permo-Carboniferous temnospondyl *Archegosaurus decheni* Goldfuss, 1847 from the Saar-Nahe Basin, Germany. Trans Roy Soc Edin Earth Sci 2006;96:131-162.

Witzmann F.. The stratigraphically oldest eryopoid temnospondyl from the Permo-Carboniferous Saar-Nahe Basin, Germany. Paläontol Zeit 2012;88:1-9.

Young GC, Long JA, Ritchie A. Crossopterygian fishes from the Devonian of Antarctica: systematics, relationships, and biogeographic significance. Rec W Austral Mus Suppl 1992;14:1–77.

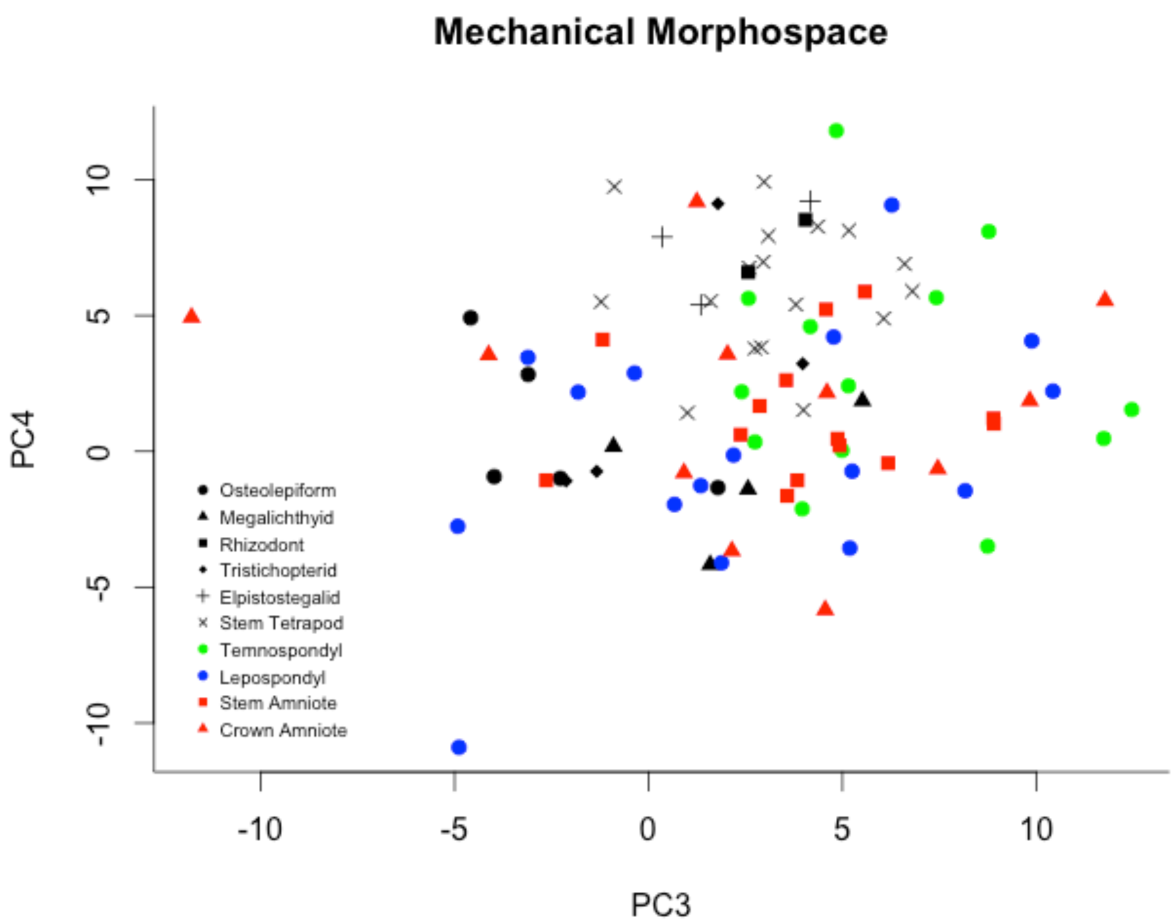

Figure S8. Biomechanical morphospace showing the distribution of all taxa on PCs 3 and 4.

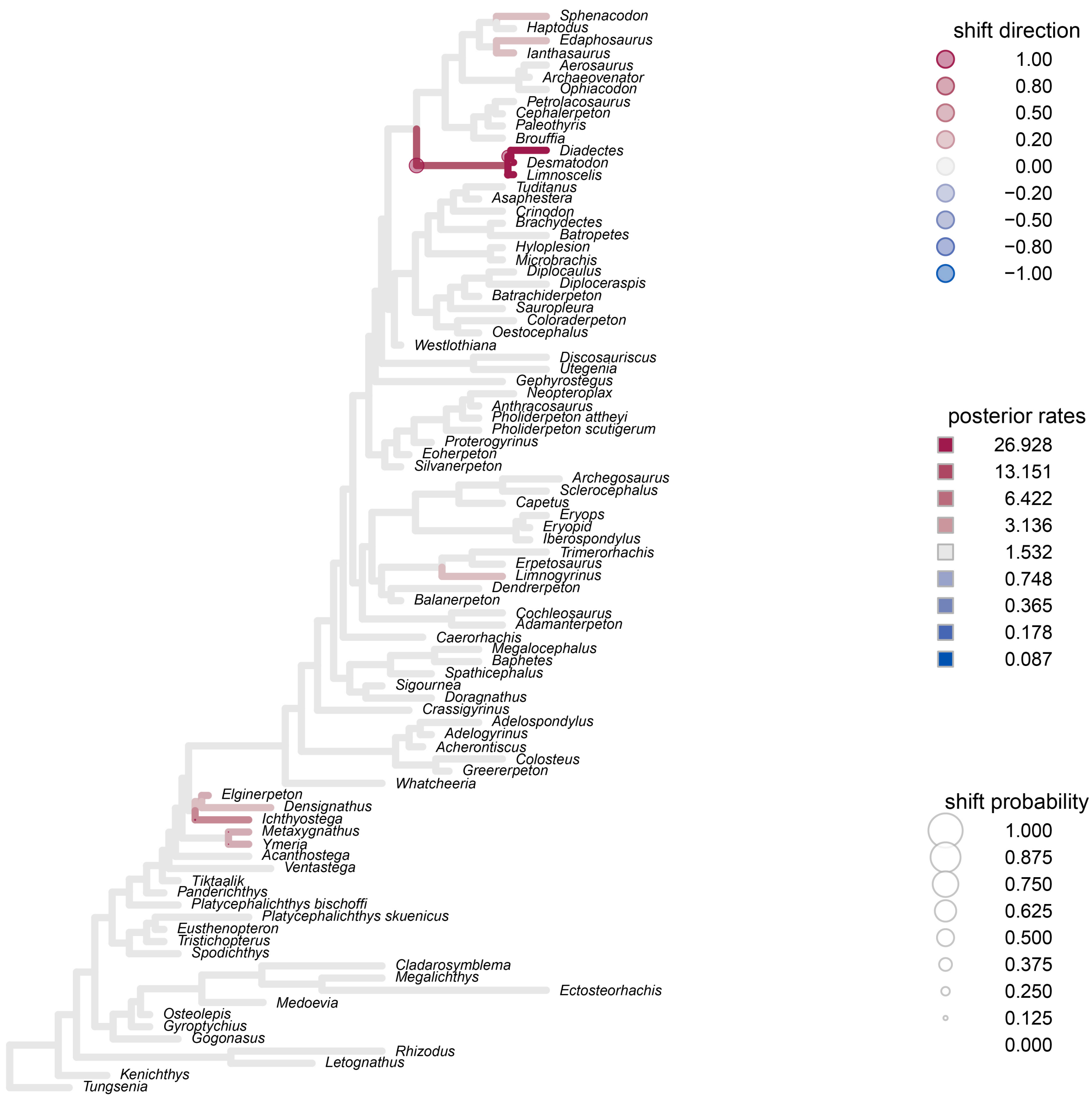

Figure S9. Inferred rates of phenotypic evolution along PC1.

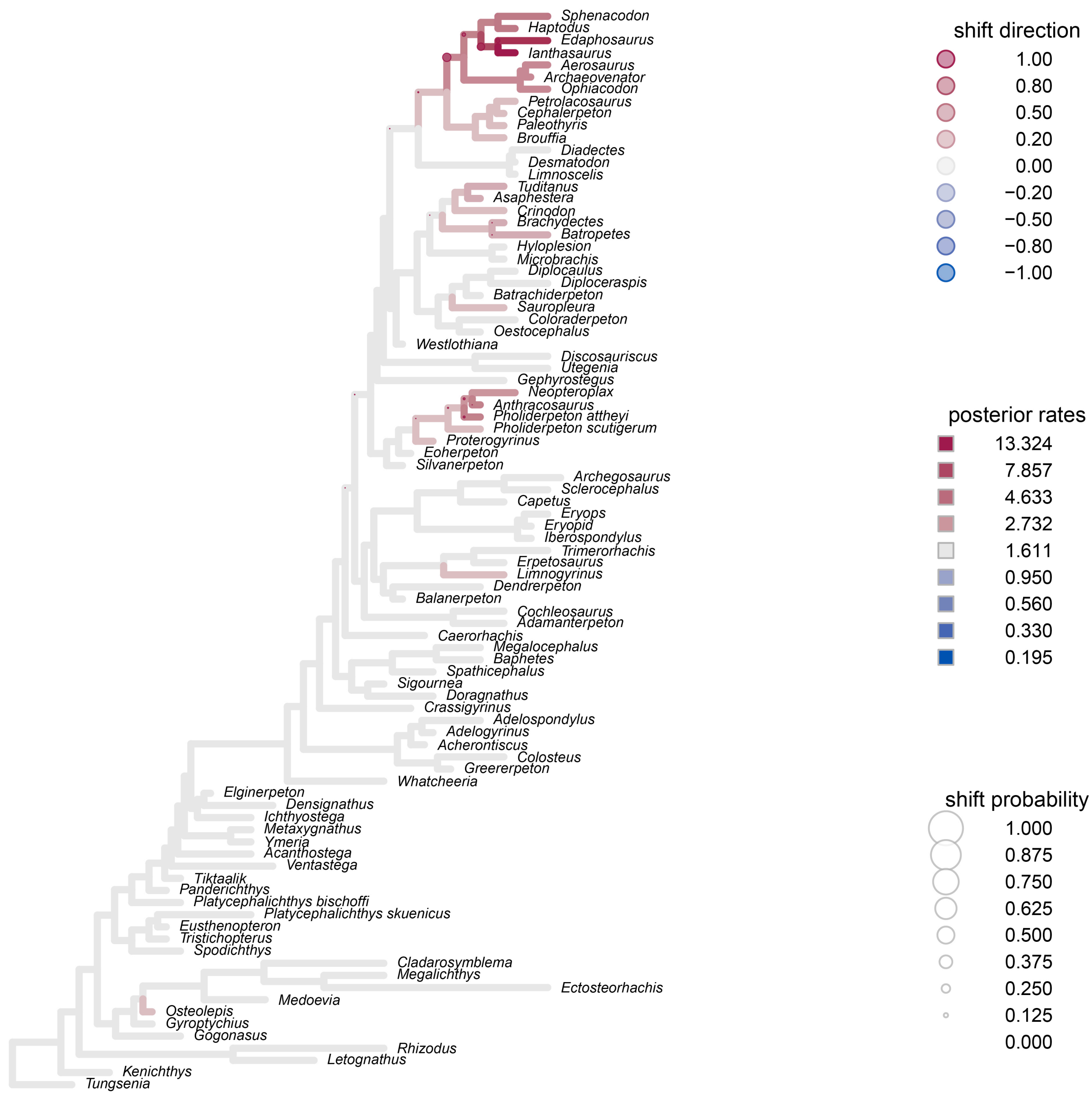

Figure S10. Inferred rates of phenotypic evolution along PC2.